Source, transport and impacts of a heavy dust event in the Yangtze River Delta, China in 2011

Xiao Fu [a,*], Shuxiao Wang [a, b,*], Zhen Cheng [a], Jia Xing [a, c], David Wong [c], Bin Zhao [a], Jiandong Wang [a], Jiming Hao [a, d]

[a] State Key Joint Laboratory of Environment Simulation and Pollution Control, School of Environment, Tsinghua University, Beijing 100084, China

[b] State Environmental Protection Key Laboratory of Sources and Control of Air Pollution Complex, Beijing 100084, China

[c] US Environmental Protection Agency, Research Triangle Park, NC, USA

[d] Collaborative Innovation Center for Regional Environmental Quality, Tsinghua University, Beijing 100084, China

*These authors contributed equally to this work

Correspondence to: S.X.Wang (shxwang@tsinghua.edu.cn)

Abstracts

Dust invasion is an important type of particle pollution in China. During 1 to 6 May in 2011, a dust event was observed in the Yangtze River Delta region (YRD). The highest PM_{10} concentration reached over 1000μg/m^3 and the visibility was below 3km. In this study, the Community Multi-scale Air Quality modeling system (CMAQ5.0) coupled with an in-line windblown dust model was used to simulate the formation, spatial and temporal characteristics of this dust event, and analyze its impacts. The threshold friction velocity for loose, fine-grained soil with low surface roughness in the dust model was revised based on Chinese data to improve the model performance. This dust storm broke out in Xinjiang and Mongolia during 28 to 30 April and arrived in the YRD region on 1 May. The transported dust particles contributed to the mean surface layer concentrations of PM_{10} in the YRD region by 78.9% during 1 to 6 May and the impacts weakened from north to south due to the removal of dust particles along the path. The dry deposition, wet deposition and total deposition of PM_{10} in the YRD reached 184.7kt, 172.6kt and 357.32kt, respectively. The dust particles also had significant impacts on optical/radiative characteristics by absorption and scattering. In Shanghai, the largest perturbations of AOD and irradiance were about 0.8DU and -130 W/m^2, which could obviously influence the radiation balance in this region. The decrease of actinic fluxes future impacts the photochemistry. In Shanghai, the negative effects on the NO_2 and O_3 photolysis could be -35% when dust particles arrived. The concentrations of O_3 and OH were reduced by 1.5% and 3.1% in the whole China, and by 9.4% and 12.1% in the YRD region, respectively. The change of O_3 and OH level can future affect the formation of secondary aerosols in the atmosphere by directly determines the oxidation rate of their precursors. The work of this manuscript is meaningful for understanding the dust emissions in China as well as for the application of CMAQ in Asia. It is also helpful to understand the formation mechanism and impacts of dust pollution in the YRD.

1 Introduction

Mineral dust is the largest single contributor to particulate matter in the atmosphere (Forster et al., 2007; Rind et al., 2009). China is one of regions which are usually affected by dust storms, especially in spring. The dust particles mainly originate from deserts in northern China and Mongolia (Zhang et al., 2003), which can reach Taiwan, southern China, Korea and even North America (Ault et al., 2011; Fan et al., 2013; Lin et al., 2012; Park et al., 2013). Suspended dust particles can be transported a long distance as carriers and reaction sites of many harmful species, such as fungal spores, microorganisms and anthropogenic pollutants including NO_X, VOC, and Pb (Huang et al., 2010; Lee et al., 2009). Some studies showed that the number of people with lung inflammation or stroke increased significantly during dust storm episode (Ichinose et al., 2008; Kang et al., 2013). It can also impact the radiation directly by absorption and scattering (Sokolik et al., 2001; Sun et al., 2012), and indirectly serve as cloud condensation nuclei (CCN) (Smoydzin et al., 2012; Solomos et al., 2012). Finally, dust particles can be removed by dry and wet depositions, which can take new nutrients into the surface water and may also result in acidification (Doney et al., 2007; Shi et al., 2012).

Numerical modeling is a useful method to analyze the characteristics of a dust event. In the recent decade, numerous physical or empirical based numerical models have been developed to describe the formation and transport of dust particles (e.g. Han et al., 2004; Wang et al., 2012a; Zender et al., 2003). They are usually implemented into air quality or climate models and used to analyze the impacts of dust particles on air quality, biogeochemical cycling, climate, and so on (Han et al., 2012; Wang et al., 2010a; Yan et al., 2012).The Community Multi-scale Air Quality modeling system (CMAQ) developed by the United States Environmental Protection Agency (US EPA) is one of the widely-used air quality models (Knipping et al., 2006; Wang et al., 2010c; Wang et al., 2012b). Wang et al. (2012a) implemented an online dust emission and heterogeneous chemistry module into CMAQ version 4.7. Tong et al. (2011,submitted) developed a dust emission model called FENGSHA and used it to estimate the dust emission in the United States. Based on Tong's work, the dust model was coupled with the newest version of CMAQ (CMAQ5.0) and

was officially released in February of 2012 (http://www.cmaq-model.org/). Up to now, this model has been used in the US only and the performance in other regions, especially in East Asia, still need to be evaluated.

The Yangtze River Delta (YRD), located in the eastern part of China, is one of China's most developed and densely populated regions. This region covers 213340km^2, only about 2.22% of China's territory. However, A few metropolitan cities such as Shanghai, Nanjing, Suzhou, and Hangzhou locate in the YRD. Therefore, it lives 11.65% of the national population, produces 21.51% of the GDP, consumes 16.57% of the national energy and bears 16.26% of the total vehicle population in 2010 (National Bureau of Statistics of China, 2011a; 2011b). Previous observations have indicated the long range transport of dust particles may significantly contribute to the particulate pollution in Shanghai, the largest mega-city in this area (Huang et al., 2010; Fu et al., 2010). Therefore, it is necessary to quantify the impacts of dust transport on regional air quality in the YRD region.

In this paper, we analyzed a strong dust event observed in the YRD region during 1 to 6 May of 2011 using the CMAQ5.0 with an in-line windblown dust model. In the next section, a detailed description of model system is presented. Section 3 evaluates the model performance on meteorological conditions and pollutants concentration predictions. A further analysis of this dust event, including the dust emission characteristics, meteorological conditions, dust transport, effects of dust on deposition and photochemistry is presented in section 4. Major findings and conclusions are summarized in Section 5.

2 Model description

2.1 Simulation domain and episode

One-way triple nesting simulation domains are used in this study, as shown in **Fig.1.** They are based on the Lambert projection with the two true latitudes of 25°N and 40°N. Domain 1 covers most of China with a grid resolution of 36km×36km; Domain 2 covers the eastern China with a grid resolution of 12km×12km; Domain 3 covers the Yangtze River Delta region with a grid resolution of 4km×4km. From 1 May of 2011, an obvious increase

of the PM concentration in the YRD region was observed. The highest PM_{10} concentration reached over 1000μg/m^3 and the visibility decreased from above 10km to below 3km. The $PM_{2.5}/PM_{10}$ ratio was only 25%, which may be affected by dust storm. Considering the transport of dust, the simulation episode chosen is from 28 April to 6 May in 2011.

2.2 CMAQ model configurations and inputs

The Community Multi-scale Air Quality modeling system version 5.0 (CMAQ5.0) with the updated 2005 Carbon Bond gas-phase mechanism (CB05) and the AERO6 aerosol module was applied in this study, which was officially released in February 2012. CB05 is enhanced by using the updated toluene chemistry (Whitten et al., 2010), modifying rate constants for N_2O_5 hydrolysis and adding reactions of xylene and toluene with chlorine radical. For aerosol module, AERO6 reflects many new features and improvements over AERO5. The enhancements include splitting primary $PM_{2.5}$ emissions into 18 species; incorporation of ISORROPIAv2.1 (Fountoukis and Nenes, 2007); update of primary organic aerosol (POA) aging (Simon and Bhave, 2012); addition of a new in-line windblown dust model (Tong et al.,2011 submitted); update of secondary organic aerosol (SOA) yield parameterization.

The Weather Research & Forecasting Model (WRF) version 3.3.1 was used to generate the meteorological fields. The first guess fields were obtained from final operational global analysis data of the National Center for Environmental Prediction (NCEP). The Automated Data Processing (ADP) data was used to the analysis of four-dimensional data assimilation (FDDA). The physical options used in the WRF model were Morrison double-moment microphysics scheme (Morrison et al., 2009), the Rapid Radiative Transfer Model for GCMs (RRTMG) shortwave and longwave radiation scheme (Mlawer and Clough., 1998; Mlawer et al., 1997), Pleim-Xiu land surface scheme (Xiu and Pleim., 2001), ACM2 PBL scheme (Pleim, 2007), and Kain-Fritsch cumulus scheme (Kain., 2004).

In this study, the anthropogenic emission inventory was developed based on the information provided by Fu et al. (2013), Zhao et al. (2013), and the Trace-P emissions (Streets et al., 2003). For the YRD region (including Jiangsu, Zhejiang and Shanghai), the data were mainly from Fu et al. (2013), which is with higher spatial resolution than the

emission in Zhao et al and TRACE-P. For other provinces in China except for the YRD, the data were from Zhao et al. (2013). For other Asian countries, TRACE-P dataset was used. The biogenic emissions were calculated by the Model of Emissions of Gases and Aerosols from Nature (MEGAN) (Guenther et al., 2006). The total emissions for major pollutants (not including dust emissions) are listed in **Table 1**.

In order to evaluate the performance of the dust model and the impacts of dust emissions, three simulations are conducted in this study, including DUST_DEFAULT, DUST_REVISED and DUST_OFF. As shown in **Table 2**, here DUST_DEFAULT means the situation that the dust model with officially-released parameters is used. It is designed to evaluate the performance of the default dust model for this dust event. For DUST_REVISED, parameters including the threshold friction velocity for loose, fine-grained soil with low surface roughness and $PM_{2.5}/PM_{10}$ ratio are chosen based on Chinese measurement data. In order to analyze the impacts of dust, another simulation (DUST_OFF) is also conducted, which refers to the situation that the dust model is turned off.

2.3 The in-line windblown dust model in CMAQ5.0

The dust emissions were generated by the new in-line windblown dust model in CMAQ5.0 (Tong et al., 2011 submitted). The vertical flux F (gm^{-2} s^{-1}) was calculated by the following formula:

$$F = \sum_{i,j} K \times A \times \frac{\rho}{g} \times S_i \times SEP \times u_* \times (u_*^2 - u_{*ti,j}^2) \text{ for } u_* > u_{*t} \qquad (1)$$

Where i is the type of erodible lands, including shrub land, shrub grass and barren land; j is the soil types. Different soil types have different fractions of clay, silt and sand; K represents the ratio of vertical flux to horizontal sediment flux, which is associated with the clay content (%) and calculated by the following formula (Marticorena and Bergametti, 1995; Tong et al., 2011 submitted):

$$K = \begin{cases} 10^{0.134[clay\%]-6} & for \quad clay\% < 20\% \\ 0.0002 & for \quad clay\% \geq 20\% \end{cases} \qquad (2)$$

A is the particle supply limitation; ρ is the air density; g is gravitational constant; S (m^2) is

the area of dust source, which is based on the MODIS land use data. For the three erodible land types, it assumes that the fraction of erodible lands capable of emitting dust is 0.5, 0.25 and 0.75, respectively; SEP is the soil erodibility factor, which is determined by the following formula:

$$SEP = 0.08 \times clay\% + 1.00 \times silt\% + 0.12 \times sand\% \quad (3)$$

u_* (m/s) is the friction velocity, which directly comes from the output of WRF.

In this equation, u_{*_t} is the threshold friction velocity, which controls the intensity and the onset of dust emissions. It is expressed by $u_{*ti.j} = u'_{*ti,j} \times f_{di,j} \times f_{mi,j}$, considering the effects of surface roughness ($f_{di,j}$), soil moisture and snow cover ($f_{mi,j}$). $u'_{*ti,j}$ is the threshold friction velocity for loose, fine-grained soil with low surface roughness. The default value of $u'_{*ti,j}$ is based on the measurement results of dust samples from the Mojave Desert in America (Gillette et al., 1980) and the average value is 0.7, which is used in the simulation of DUST_DEFAULT. For the simulation DUST_REVISED, it was chosen as 0.3 based on the measurement results of dust samples from the northern desert in China (Li et al., 2007). Besides, different from the default value, the $PM_{2.5}/PM_{10}$ ratio for dust emission was chosen as 0.1 (Niu et al., 2003; Wang et al., 2012a). For other parameters, the default values in the model were used.

3 Model evaluation

3.1 Evaluation of meteorological simulations

The accuracy of the meteorological prediction is the foundation of air quality simulation. **Table 3** summarizes the statistical performance of 10-m wind speed and wind direction (WS10 and WD10, respectively), 2-m temperature (T2) and 2-m humidity (H2). Here, the simulated wind direction was calculated based on U-wind speeds (uu) and V-wind speeds (vv). Its range is $0 \le wind\_direction < 360\,\text{degree}$ and it had an unique value. Hourly or every third hour observation data were obtained from the National Climatic Data Center

(NCDC) for 1955 stations within Domain 1, 787 stations within Domain 2 and 90 stations within Domain 3. The statistical parameters contain mean observation (Mean OBS), mean simulation (Mean SIM), bias, gross error (GE), root mean square error (RMSE), and the index of agreement (IOA), which are explained in details in Baker (2004). The benchmark values are suggested by Emery et al. (2001), which are based on results of many studies in US. These values are also used as reference standards in this study.

As shown in **Table 3**, the performance of WS10 is satisfactory. The bias, GEs, RMSEs and IOA values of all the three domains are within the benchmark range. For WD10, while the biases are below the 10 degrees, the gross errors are 2 to 21 degrees higher than the benchmark value. The high gross errors may result from a caveat in treating the wind direction vector as a scalar in the calculation method, as described in previous studies (Wang et al., 2010b; Zhang et al., 2006). The T2 predictions were slightly underestimated. But the IOA values for all three domains are close to one, indicating an acceptable performance. The results for Domain 1 (36-km grid) are relatively worse, which mainly result from the poor representation of steep terrains with a coarse grid resolution (Wang et al., 2012a). For humidity, generally the model can reproduce the observed values. For Domain 2 (12-km grid) and Domain 3 (4-km grid), all statistical parameters are within the benchmark range. For Domain 1 (36-km grid), the bias and GE values is above the benchmark, but the IOA value is a little lower. Because the benchmark values are mostly based on the domains with 4-km or 12-km resolution and the meteorological predictions can be more accurate than that for 36-km, this slight underestimation is acceptable. Because the dust storm formation and transport are affected significantly by wind, we further compare wind speed and wind direction between observations and predictions at the 3 monitoring sites (see **Fig.S1**),which are in the source region, along the transport path and in the downwind region, respectively.

3.2 Evaluation of chemical variables

3.2.1 Evaluation of pollutants concentration predictions

Two observational datasets were used for model evaluation of pollutants concentration predictions. The first one is the hourly PM_{10} concentration for official monitoring sites in

Mainland China obtained from the Ministry Environmental Protection of the People's Republic of China (MEP) (http://113.108.142.147:20035/emcpublish/). Considering that the data of some monitoring sites are missing during this simulation episode, 546 monitoring sites (as shown in **Fig.1**) were chosen for the model evaluation. Another dataset was from the field measurement by Tsinghua University for 3 monitoring sites in the YRD region (as shown in **Fig. 2**), including Shanghai city, Nanjing in Jiangsu Province and Ningbo in Zhejiang Province.

Table 4 shows the hourly PM_{10} concentrations from observations and simulations DUST_OFF, DUST_DEFAULT and DUST_REVISED for all 3 domains. The results of DUST_OFF underestimate the PM_{10} concentration significantly, with the Normalized Mean Bias (NMBs) of -47.1%, -37.8% and -72.2% for the Domain 1, 2, and 3, respectively. Compared with the results of DUST_OFF, the model performance of DUST_DEFAULT was not improved substantially. The model performance of DUST_REVISED is significantly improved compared with that of DUST_DEFAULT. The NMBs for Domain 1, 2, and 3 are -10.9%, 7.1% and -13.6%, respectively. The correlation coefficients (R) are at the range of 0.4-0.6. **Figure S2** shows the comparison of the spatial distribution for the PM_{10} concentrations. In general, the spatial distribution of the observations was consistent with the simulations, especially near the source region (like 29 and 30 April). We can also see some overestimated cases at downwind regions. The possible reason is that the simulated results are average values for 36km grid and it's difficult to capture the specific concentration for every point accurately for some time.

In order to test the model performance in terms of the ability to reproduce dust emission better, we compared PM_{10} concentration between observations and predictions at the 3 sites near source region, which include Baotou in Inner Mongolia (109.85E, 40.68N), Jinchang in Gansu (102.19E, 38.52N) and Yinchuan in Ningxia (106.17E, 38.48N). The comparison of observed and simulated hourly PM_{10} concentration is shown in the **Fig.S3**. Compared with DUST_DEFAULT and DUST_OFF, the model performance for DUST_REVISED is improved significantly. The NMBs for Baotou, Jinchang and Yinchuan are -22.2%, -38.6% and -50.4% averagely during 28 April to 6 May. The R values for these three sites are 0.77, 0.66 and 0.59, respectively. The revised model can generally capture the dust outbreak event

during 29 and 30 April.

In order to evaluate the performance of DUST_REVISED further, we compared the temporal variations of simulated hourly PM_{10} and $PM_{2.5}$ concentration with observations in 3 monitoring sites in the YRD region (as shown in **Fig. 2**). From 1 to 4 May, a strong dust event occurred in this region and the highest PM_{10} concentration could reach more than 1000μg/m^3. In general, the model could reproduce the temporal trends and high PM_{10} concentrations well. The NMBs of PM_{10} predictions for Nanjing, Shanghai and Ningbo are -17%, -35% and 4%, respectively, and the correlation coefficients (R) are about 0.65-0.85. Relative large deviations occur at a few moments (e.g. early of May 2 in Nanjing, early of May 3 in Shanghai and middle of May 2 in Ningbo), which may result from the poor prediction of wind speed or wind direction at these moments. For example, at early time of May 3 in Shanghai, the simulated wind direction is 20-40 degree, but the observed wind direction is 90-180 degree. On 3 May, dust particles were transported from sea to land and therefore this deviation of wind direction may lead to the underestimation of PM in Shanghai. For the $PM_{2.5}$ concentration, the model could reproduce its variation trend well and the correlation coefficients (R) are about 0.6-0.8. However, the model tends to overestimate the $PM_{2.5}$ concentration slightly, with NMBs of 14%, 28% and 41% for Nanjing, Shanghai and Ningbo, respectively. This overestimation may be affected by the splitting between $PM_{2.5}$ and $PM_{2.5-10}$, because we just simply allocate 10% of dust PM_{10} emission to $PM_{2.5}$. Anyway, the comparison results demonstrate the CMAQ5.0 with the revised dust module could capture the PM variation reasonably well.

3.2.2 Evaluation of aerosol optical depth (AOD) predictions

Figure 3 compares the temporal variations of observed daily average AOD column from AERONET and predictions from DUST_REVISED at two sites. The Beijing site (116.38E, 39.98N) is located at the transport path of dust and the Taihu site (120.21E, 31.42N) is in the YRD region. The comparisons for the sites near the dust source region are not included, because the measurement data at these sites are missing during this episode. As shown in **Fig.3**, the simulated AOD agrees well with the observations. The NMBs for Beijing and

Taihu site are 5.4% and 17.8%, respectively. This demonstrated the ability of DUST_REVISED in capturing both the day-to-day variations of aerosols including dust particles.

Figure S4 presents the daily averaged AOD distributions derived from simulation and retrieved from MODIS during the dust event. The comparison shows that the simulated AOD can generally catch the spatial distribution of satellite observation over Eastern China.

4 Results and discussion

4.1 Dust emission

The simulation results of DUST_REVISED indicated that about 695kt dust particles (PM_{10}) were emitted in Xinjiang and Mongolia during 28 to 30 April, 2011. **Fig. 4** and **Fig. 5** show the spatio-temporal characteristic of dust emissions. On 28 April, a large amount of dust particles (about 145kt) were generated up in Xinjiang Province and southwestern Mongolia by the strong northwestern wind. On 29 April, more new dust particles (about 515kt) were emitted in south Mongolia and the highest density of dust emission could reach above $7t/km^2$. The largest value of total dust emission for the whole region occurred at 1500 BJT on 29 April, about 66.8kt/h. Another small amount of dust particles were emitted on 30 April, only about 35kt. As shown in **Fig.5**, the predicted total dust emissions based on DUST_DEFAULT were only about 11kt and underestimated by 98% compared with that of DUST_REVISED. The default threshold friction velocity for loose, fine-grained soil with low surface roughness (about 0.7) was too high for Asian dust sources.

4.2 Analysis of metrological condition for this dust event

As shown in **Fig.6 (a)** and **Fig.6 (b)**, on 28 April, a cyclone was formed in the Mongolia, associating with a cold front in the rear part of the low-pressure system. Strong surface winds (8-14m/s) occurred in eastern Xinjiang and western Mongolia, generating a dust storm there. On 29 April, the low-pressure cyclone developed further and moved toward east to the middle-southern Mongolia (as shown in **Fig.6 (c)** and **(d)**). The strong horizontal wind flow

and the vertical flow caused the uplifting of dusts in this region. These possible locations of dust storms are in accordance with the satellite observations (http://www.temis.nl/airpollution/absaai/absaai-gome2a.php?year=2011&datatype=pics&freq=daily). Due to the influence from the low pressure system, the high pressure associated with cold air arrived in the YRD region on 1 May (as shown in **Fig.6 (e)** and **(f)**). From 1 May, the pressure and wind speed began to increase, and the temperature began to decrease. As shown in **Fig.7**, the pressure in Shanghai increased from 1003.5mb on 1 May to 1016mb on 3 May, and the temperature decreased by 5-10 degree Celsius. When the upper-level trough was leading the approach of cold air from north to south, dust particles also arrived in the YRD and the PM_{10} concentration in Shanghai increased from 74μg/m^3 to 800μg/m^3 on 1 May (as shown in **Fig.2**). Controlled by high pressure, the wind became relatively light from the midday of 3 May, which is adverse to the dispersion of dust particles. The tail of the cold front passed over the YRD region at the end of 4 May. The temperature and wind speed began to increase, the pressure began to decrease.

4.3 Dust transport and its impacts on PM_{10} concentration

Fig.8 shows the spatio-temporal variation of PM_{10} concentration differences between DUST_REVISED and DUST_OFF, which helps to understand the transport of this dust event and the impacts of dust storm on PM_{10} concentration. The emitted dust particles mixed together and moved on toward eastern and southern direction. The PM_{10} concentration at the sites near the dust sources, i.e. Lanzhou city in Gansu Province, could reach nearly 5000μg/m^3. On 30 April, the dust began to affect the eastern and central China. For example, the PM_{10} concentration in Tianjin city increased from 50μg/m^3 to 1100μg/m^3. The dust band arrived in the YRD on 1 May and the PM_{10} concentration in Shanghai increased from 50μg/m^3 to 640μg/m^3 (as shown in **Fig. 2**). The maximum PM_{10} value reached 1000μg/m^3 on 2 May. Another part of the dust band also reached Korea and even Japan, but was blew back to the YRD by the southwestern wind on 3 May. This pathway of dust is similar with the dust storm observed in Shanghai in 2007 (Fu et al., 2011), which is one of the typical dust pathways that lead to heavily polluted days in the YRD due to dust transport. From 4 May,

the impact of dust on the YRD region began to decline. By comparing the simulation results of DUST_REVISED and DUST_OFF, the contribution of the dust emissions to the mean surface layer concentrations of PM_{10} in the YRD region is 78.9% during 1 to 6 May and the impacts weakened from north to south due to the deposition of dust particles along the path. This contribution ratio was comparable with the ground measurement in Shanghai during a dust storm in 2009, which was 76.8% (Huang et al., 2012).

4.4 Deposition of dust aerosols in the YRD region

Dust particles can be finally removed by dry and wet depositions. During 1 to 6 May, the dry deposition, wet deposition and total deposition of PM_{10} were 184.7kt, 172.6kt and 357.32kt, respectively, of which $PM_{2.5}$ depositions accounted for 5.7%, 36.4% and 20.5%, respectively. **Fig.9** shows the spatial distribution of dry deposition (DDEP), wet deposition (WDEP), total deposition (TDEP) and the difference of total deposition between DUST_REVISED and DUST_OFF situation (TDEP_DIFF) for PM_{10} in the Domain 3 (covering the YRD region) in these six days.

The dry depositions of PM_{10} accounted for 51.7% of the total. In general, the dry depositions in Jiangsu Province and Shanghai city were larger than that in Zhejiang Province, which was affected by the PM_{10} concentration. Dust particles were transported from north to south and the concentration became lower at the end of the transport path. Meanwhile, relatively high values can also be seen at some urban or forest regions. Besides the impacts of PM_{10} concentration, the larger associated parameters (e.g. the surface roughness length and leaf-area index) can lead to higher deposition velocity (Kumar et al., 2008; Fan et al., 2009). As shown in **Fig.9**, wet depositions mainly occur in East Sea, Shanghai, southern Zhejiang etc. Besides the impacts of PM_{10} concentration, this distribution was related with the distribution of cloud and precipitation (shown as **Fig.S5**).

Comparison between the results of DUST_REVISED and DUST_OFF shows that the long range transport of dust particles increased the total deposition of PM_{10} in the YRD by 1082%, of which dry deposition increased by 2398% and wet deposition increased by 655%. These deposited particles are very harmful because of their impacts on urban environment as

well as on air quality and human health when resuspending in the atmosphere. Besides, single particle analysis in previous literatures shows that dust particles are usually rich in N (Fu et al., 2012; Geng et al., 2009), which may contribute to nitrogen deposition.

4.5 Impacts of dust storm on optical/radiative variables and photochemistry

4.5.1 Impacts on AOD and radiation

Figure 10 presents the dust impact on aerosol optical depth (AOD) and irradiance averagely during 28 April to 6 May. The average contribution of dust on AOD in the whole China is 36.5%. The high values of contribution occurred near the source region, about 1.3DU (above 90%). The strong negative effects impacts on radiative forcing mainly concentrated over the source regions where heavy dust burden and large contribution to AOD from dust, about -30 to -20W/m^2 averagely. The relatively low values of irradiance change ranging from -20 to -10 W/m^2 could be found over North China Plain and China Sea. These values are similar with the previous study (Han et al., 2012). The hourly-average simulation results showed that in Shanghai, the largest perturbations of AOD and irradiance were about 0.8DU and -130 W/m^2, which could obviously influence the radiation balance in this region.

4.5.2 Impacts on photochemistry

(1) Photolysis rates

Dust particles have important effects on photolysis rates (Bian and Zender, 2003; Ying et al., 2011). Photolysis rates (min^{-1}), also called J-values, are computed for a chemical species *w* by (Philip, 2000)

$$J_w = \int_{\lambda_1}^{\lambda_2} F(\lambda)\sigma_i(\lambda)\Phi_i(\lambda)d\lambda$$

Where, $F(\lambda)$ is the actinic flux, $\sigma_i(\lambda)$ is the absorption cross section, $\Phi_i(\lambda)$ is the quantum yield, and λ is the wavelength. $\sigma_i(\lambda)$ and $\Phi_i(\lambda)$ are unique to reactions and species. But dust can affect the actinic flux through absorption and scattering.

An online photolysis module is incorporated in CMAQ 5.0, which allows the calculation

of actinic fluxes and photolysis rates for every each grid at each time step based on the changes in particle concentrations (Binkowski et al.2007). In this study, the impacts of dust on photolysis chemistry through their effects on the actinic flux are analyzed by comparing the results of DUST_REVISED with that of DUST_OFF.

There are two important photolysis rates affecting tropospheric ozone photochemistry, the NO_2 photolysis (J[NO2]) to form the ground state oxygen atom $O(^3P)$ and the O3 photolysis (J $[O_3(O^1D)]$) to form the electronically excited $O(^1D)$ atom (Li et al., 2011):

$$O_3 + h\nu \longrightarrow O_2 + O\left(^1D\right)$$
$$NO_2 + h\nu \longrightarrow NO + O\left(^3P\right)$$

As shown in **Fig.11**, the NO_2 photolysis (J[NO2]) and the O3 photolysis (J $[O_3(O^1D)]$) as reduced by about 2.4% and 1.9% averagely in whole Domain 1 during 28 April to 6 May. The perturbations are mainly in dust source regions and along the dust transport path, which are similar with the distribution of irradiance changes.

Figure 12 shows the diurnal variation of the percentage change of J[NO2] and J$[O_3(O^1D)]$ at Shanghai in the YRD region. The reduction of J[NO2] and J$[O_3(O^1D)]$ due to dust is significant in the early morning of 2 May, nearly -40%. Besides the impacts of high dust concentration, it also indicated the effect of long aerosol optical path for incoming radiation when the solar zenith angle (SZA) is large in the morning (Li et al., 2011).

(2) Concentrations of O_3 and OH

The photolysis frequencies of J $[O_3(O^1D)]$ and J $[NO_2]$ play a key role in the formation of O_3 and OH in the troposphere through the following reactions:

$$NO_2 + h\nu \longrightarrow NO + O\left(^3P\right)$$
$$O\left(^3P\right) + O_2 + M \longrightarrow O_3 + M$$
$$O_3 + h\nu \longrightarrow O_2 + O\left(^1D\right)$$
$$O\left(^1D\right) + H_2O \longrightarrow 2OH$$
$$OH + VOCs + O_2 \longrightarrow RO_2$$
$$RO_2 + NO \longrightarrow RO + NO_2$$

The simulation results show that the surface O_3 concentrations reduced about 1.5% averagely for Domain 1 and the maximum reached 6 ppbv due to the dust storm. **Fig.13(a)**

shows that the largest perturbations of O_3 occurred in a region including China Sea, eastern China and Korea. One major reason is that air mass with dust stayed in this region for two days (May 2-3, as shown in **Fig.8**) due to the high pressure control. The average decrease of OH was about 3.1% in whole Domain 1, resulting from the reductions in O (^1D) generated by ultraviolet photolysis of O_3 (Bian and Zender, 2003). As shown in **Fig.13(b)**, the reduction of OH concentrations is correlated with the spatial distribution of J[NO_2] reduction, due to the short chemical lifetime of OH. For the YRD region, because of the reduction of local generation and long transport, the O_3 and OH concentrations were decreased by 9.4% and 12.1% averagely. These values are comparable with that reported by Ying et al. (2011), in which the O_3 reduction in Mexico City could be 10ppbv and the reduction of OH was 5-20% during a dust event. The change of O_3 and OH level can further affect the formation of secondary aerosols in the atmosphere by changing the oxidation rate of their precursors. For example, nitrate particles and sulfate particles may decrease because of the less conversion of HNO_3 from NO_2 reaction with OH, and H_2SO_4 from SO_2 reaction with OH and O_3.

5 Conclusions

In this study, we analyzed a dust event in 2011 with the CMAQ5.0 coupled with an in-line windblown dust model. The threshold friction velocity for loose, fine-grained soil with low surface roughness in the dust model was revised according to Chinese monitoring data. The predictions of the model DUST-REVISED agreed well with the observations.

This dust storm broke out in Xinjiang and Mongolia during 28 to 30 April, 2011. Dust particles were transported a long distance and the impacts even spread to the YRD region. On 1 May, the PM_{10} concentration in the YRD region began to increase and the maximum reached 1000μg/m^3. The large amount of dust particles carrying fungal spores, microorganisms and anthropogenic pollutants during transport were a serious threat to public health. At such a high population-density region, the health loss can be large. The dust particles also had significant impacts on the optical/radiative characteristics by absorption and scattering. The visibility decreased to below 3km during the dust event, which is harmful to road transportation and flight. The hourly-average simulation results showed that in Shanghai,

the largest perturbations of AOD and irradiance were about 0.8DU and -130 W/m^2, respectively. The decrease of actinic fluxes further impacts the photochemistry in this region. In Shanghai, the negative effects on the NO_2 and O_3 photolysis could be -35% when dust particles arrived. For the YRD region, because of the reduction of local generation and reduction of long range transport, the O_3 and OH concentrations are decreased by 9.4% and 12.1%. The change of O_3 and OH level can further affect the formation of secondary aerosols in the atmosphere by directly determines the oxidation rate of their precursors. For example, nitrate particles and sulfate particles may decrease because of the less conversion of HNO_3 from NO_2 reaction with OH, and H_2SO_4 from SO_2 reaction with OH and O_3.

The research about the dust pollution is an important work and modeling is a useful method. CMAQ is a wide-used air quality model and the revision of parameters for the dust emission model is meaningful for CMAQ application. Meanwhile, further studies, including more accurate particle size distributions of dust emissions, heterogeneous reactions on the surface of dust particles, the interaction between dust particle and meteorological parameters, shall be conducted to improve the understanding of dust impacts on air quality. The $PM_{2.5}/PM_{10}$ ratio for dust emission is a fixed value in the current model. But actually, it may be affected by soil texture, wind speed and so on. Secondly, the current CMAQ version does not consider about some important heterogeneous reactions on the surface of dust particles, such as SO_2, O_3, and H_2O_2, which might be an important contributor to the impacts of dust on pollutant concentration. More heterogeneous reactions shall be coupled into the model. Besides, we did not consider the effects though the feedbacks of dust on meteorology in this study. It’s meaningful to consider this effect by running the two-way WRF-CMAQ system in the future.

Acknowledgment. This work was sponsored by National Natural Science Foundation of China (21221004), Strategic Priority Research Program of the Chinese Academy of Sciences (XBD05020300), and special fund of State Key Joint Laboratory of Environment Simulation and Pollution Control (12L05ESPC). The corresponding author, Dr. Shuxiao Wang, is supported by the Program for New Century Excellent Talents in University (NCET-10-0532) and the China Scholarship Council. The authors also appreciate it very much for the help on dust emission module in CMAQ5.0 from Dr. Daniel Q. Tong at US National Oceanic and Atmospheric Administration (NOAA).

References

Ault, A. P., Williams, C. R., White, A. B., Neiman, P. J., Creamean, J. M., Gaston, C. J., Ralph, F. M., and Prather, K. A.: Detection of Asian dust in California orographic precipitation, J. Geophys. Res.-Atmos., 116, D16205, 10.1029/2010jd015351, 2011.

Baker: Meteorological Modeling Protocol for Application to PM2.5/haze/ozone Modeling Projects, 2004.

Bian, H. S., and Zender, C. S.: Mineral dust and global tropospheric chemistry: Relative roles of photolysis and heterogeneous uptake, J. Geophys. Res.-Atmos., 108, 4672, 10.1029/2002jd003143, 2003.

Binkowski, F. S., Arunachalam, S., Adelman, Z., and Pinto, J. P.: Examining photolysis rates with a prototype Online photolysis module in CMAQ, Journal of Applied Meteorology and Climatology, 46, 1252-1256, 10.1175/jam2531.1, 2007.

Doney, S. C., Mahowald, N., Lima, I., Feely, R. A., Mackenzie, F. T., Lamarque, J.-F., and Rasch, P. J.: Impact of anthropogenic atmospheric nitrogen and sulfur deposition on ocean acidification and the inorganic carbon system, Proceedings of the National Academy of Sciences of the United States of America, 104, 14580-14585, 10.1073/pnas.0702218104, 2007.

Emery, C., Tai, E., Yarwood, G.: Enhanced meteorological modeling and performance evaluation for two texas episodes. Report to the Texas Natural Resources Conservation Commission. ENVIRON, International Corp, Novato, CA, 2001.

Evans, B. T. N., and Fournier, G. R.: SIMPLE APPROXIMATION TO EXTINCTION EFFICIENCY VALID OVER ALL SIZE PARAMETERS, Applied Optics, 29, 4666-4670, 1990.

Fan, J.-l., Hu, Z. Y., Wang, T. J., and Zhou, J.: Dynamics of dry deposition velocities of atmospheric nitrogen compounds in a broadleaf forestland, China Environmental Science, 29, 574-577, 2009.

Fan, Q., Shen, C., Wang, X. M., Li, Y., Huang, W., Liang, G. X., Wang, S. Y., and Huang, Z. E.: Impact of a dust storm on characteristics of particle matter (PM) in Guangzhou, China, Asia-Pac. J. Atmos. Sci., 49, 121-131, 10.1007/s13143-013-0013-2, 2013.

Forster, P., Artaxo, P., Berntsen, T., Betts, R., et al.: Changes in atmospheric constituents and in radiative forcing. In: Climate Change 2007: The Physical Science Basis. Contribution of Working Group I to the Fourth Assessment Report of the Intergovernmental Panel on Climate Change, edited by: Solomon,S., Qin, D., Manning, M., Chen, Z., Marquis, M., Avert, K. B.,Tignor, M., andMiller, H. L., Cambridge University Press, Cambridge,United Kingdom and New York, NY, USA, 2007.

Fountoukis, C., and Nenes, A.: ISORROPIA II: a computationally efficient thermodynamic equilibrium model for K+-Ca2+-Mg2+-Nh(4)(+)-Na+-SO42--NO3--Cl--H2O aerosols, Atmospheric Chemistry and Physics, 7, 4639-4659, 2007.

Fu, H., Zhang, M., Li, W., Chen, J., Wang, L., Quan, X. and Wang, W.: Morphology, composition and mixing state of individual carbonaceous aerosol in urban Shanghai. Atmos. Chem. Phys., 12, 693–707, 2012.

Fu, Q., Zhuang, G., Li, J., Huang, K., Wang, Q., Zhang, R., Fu, J., Lu, T., Chen, M., Wang,

Q., Chen, Y., Xu, C., and Hou, B.: Source, long-range transport, and characteristics of a heavy dust pollution event in Shanghai, J. Geophys. Res.-Atmos., 115, D00k29, 10.1029/2009jd013208, 2010.

Fu, X., Wang, S. X., Zhao, B., Xing, J., Cheng, Z., Liu, H., and Hao, J. M. : Emission inventory of primary pollutants and chemical speciation in 2010 for the Yangtze River Delta region, China, Atmospheric Environment, 70, 39-50, 10.1016/j.atmosenv.2012.12.034, 2013.

Geng, H., Park, Y., Hwang, H., Kang, S., and Ro, C.-U.: Elevated nitrogen-containing particles observed in Asian dust aerosol samples collected at the marine boundary layer of the Bohai Sea and the Yellow Sea, Atmos. Chem. Phys., 9, 6933–6947, doi:10.5194/acp-9-6933-2009, 2009.

Gillette, D., J. Adams, A. Endo, D. Smith, and R. Kihl.: Threshold Velocities for Input of Soil Particles Into the Air by Desert Soils, J. Geophys. Res., 85(C10), 5621-5630, 1980.

Guenther, A., Karl, T., Harley, P., Wiedinmyer, C., Palmer, P. I., and Geron, C.: Estimates of global terrestrial isoprene emissions using MEGAN (Model of Emissions of Gases and Aerosols from Nature), Atmospheric Chemistry and Physics, 6, 3181-3210, 2006.

Han, X., Ge, C., Tao, J. H., Zhang, M. G., and Zhang, R. J.: Air Quality Modeling for a Strong Dust Event in East Asia in March 2010, Aerosol Air Qual. Res., 12, 615-628, 10.4209/aaqr.2011.11.0191, 2012.

Han, Z. W., Ueda, H., Matsuda, K., Zhang, R. J., Arao, K., Kanai, Y., and Hasome, H.: Model study on particle size segregation and deposition during Asian dust events in March 2002, J. Geophys. Res.-Atmos., 109, D19205, 10.1029/2004jd004920, 2004.

Huang, K., Zhuang, G., Li, J., Wang, Q., Sun, Y., Lin, Y., and Fu, J. S.: Mixing of Asian dust with pollution aerosol and the transformation of aerosol components during the dust storm over China in spring 2007, J. Geophys. Res.-Atmos., 115, D00k13, 10.1029/2009jd013145, 2010.

Huang, K., Zhuang, G., Lin, Y., Fu, J.S., Wang, Q., Liu, T., Zhang, R., Jiang, Y., Deng, C., Fu, Q., Hsu, N.C., and Cao, B.: Typical types and formation mechanisms of haze in an Eastern Asiamegacity, Shanghai, Atmospheric Chemistry and Physics, 12, 105–124, doi:10.5194/acp-12-105-2012, 2012.

Ichinose, T., Yoshida, S., Hiyoshi, K., Sadakane, K., Takano, H., Nishikawa, M., Mori, I., Yanagisawa, R., Kawazato, H., Yasuda, A., and Shibamoto, T.: The effects of microbial materials adhered to Asian sand dust on allergic lung inflammation, Archives of Environmental Contamination and Toxicology, 55, 348-357, 10.1007/s00244-007-9128-8, 2008.

Kain, J. S.: The Kain-Fritsch convective parameterization: An update, Journal of Applied Meteorology, 43, 170-181, 10.1175/1520-0450(2004)043<0170:tkcpau>2.0.co;2, 2004.

Kang, J. H., Liu, T. C., Keller, J., and Lin, H. C.: Asian dust storm events are associated with an acute increase in stroke hospitalisation, J. Epidemiol. Community Health, 67, 125-131, 10.1136/jech-2011-200794, 2013.

Knipping, E. M., Kumar, N., Pun, B. K., Seigneur, C., Wu, S. Y., and Schichtel, B. A.: Modeling regional haze during the BRAVO study using CMAQ-MADRID: 2. Source region attribution of particulate sulfate compounds, J. Geophys. Res.-Atmos., 111, D06303, 10.1029/2004jd005609, 2006.

Kumar, R., Srivastava, S. S., and Kumari, K. M.: Modeling dry deposition of S and N compounds to vegetation, Indian Journal of Radio & Space Physics, 37, 272-278, 2008.

Lee, S., Choi, B., Yi, S. M., and Ko, G.: Characterization of microbial community during Asian dust events in Korea, Sci. Total Environ., 407, 5308-5314, 10.1016/j.scitotenv.2009.06.052, 2009.

Li, G., Bei, N., Tie, X., Molina, L.T.: Aerosol effects on the photochemistry in Mexico City during MCMA-2006/MILAGRO campaign, Atmos. Chem. Phys., 11, 5169–5182, 2011.

Li, W. Y., Shen, Z.B, Lu, S.H, Li, Y.H: Sensitivity Tests of Factors Influencing Wind Erosion, JOURNAL OF DESERT RESEARCH, 27, 984-993, 2007.

Lin, C. Y., Chou, C. C. K., Wang, Z. F., Lung, S. C., Lee, C. T., Yuan, C. S., Chen, W. N., Chang, S. Y., Hsu, S. C., Chen, W. C., and Liu, S. C.: Impact of different transport mechanisms of Asian dust and anthropogenic pollutants to Taiwan, Atmospheric Environment, 60, 403-418, 10.1016/j.atmosenv.2012.06.049, 2012.

Mlawer, E. J., Taubman, S. J., Brown, P. D., Iacono, M. J., and Clough, S. A.: Radiative transfer for inhomogeneous atmospheres: RRTM, a validated correlated-k model for the longwave, J. Geophys. Res.-Atmos., 102, 16663-16682, 10.1029/97jd00237, 1997.

Mlawer, E. J., and Clough, S. A.: Shortwave Clear-Sky Model-Measurement Intercomparison Using RRTM, the 8th Atmospheric Radiation Measurement (ARM) Science Team Meeting, Tucson, Arizona, USA, 1998,

Morrison, H., Thompson, G., and Tatarskii, V.: Impact of Cloud Microphysics on the Development of Trailing Stratiform Precipitation in a Simulated Squall Line: Comparison of One- and Two-Moment Schemes, Mon. Weather Rev., 137, 991-1007, 10.1175/2008mwr2556.1, 2009.

National Bureau of Statistics of China, 2011a.China Statistical Yearbook2011. China Statistics Press, Beijing.

National Bureau of Statistics of China, 2011b.China Energy StatisticalYearbook2011. China Statistics Press, Beijing.

Niu, S. J., and Sun, Z. B.: Aircraft observation of spatial and temporal characteristics of desert dust aerosol and PM2.5 Annual Meeting of Chinese Meteorological Society Beijing, 2003, 55-56-57-58,

Park, S.U., Choe, A., and Park, M.S.: A simulation of Asian dust events observed from 20 to 29 December 2009 in Korea by using ADAM2, Asia-Pac. J. Atmos. Sci., 49, 95-109, 10.1007/s13143-013-0011-4, 2013.

Philip J. C., Incorporation of Non-Linear Effective Cross-Section Parameterizations into a Fast Photolysis Computation Code (Fast-J), Journal of Atmospheric Chemistry, 37**:** 283–297, 2000.

Pleim, J. E.: A combined local and nonlocal closure model for the atmospheric boundary layer. Part I: Model description and testing, Journal of Applied Meteorology and Climatology, 46, 1383-1395, 10.1175/jam2539.1, 2007.

Rind, D., Chin, M., Feingold, G., Streets, D., Kahn, R. A.,Schwartz, S. E., and Yu, H.: Modeling the effects of aerosolson climate, in atmospheric aerosol properties and climate impacts, A Report by the US Climate Change Science Program andthe Subcommittee on Global Change Research, edited by: Chin,M., Kahn, R. A., and

Schwartz, S. E., National Aeronautics andSpace Administration, Washington, DC, USA, 2009.

Shi, J.H., Gao, H.W., Zhang, J., Tan, S.C.,Ren, J.L., Liu, C.G., Liu, Y., and Yao, X.: Examination of causative link between a spring bloom and dry/wet deposition of Asian dust in the Yellow Sea, China, J. Geophys. Res.-Atmos., 117, D17304, 10.1029/2012jd017983, 2012.

Simon, H., and Bhave, P. V.: Simulating the Degree of Oxidation in Atmospheric Organic Particles, Environmental Science & Technology, 46, 331-339, 10.1021/es202361w, 2012.

Smoydzin, L., Teller, A., Tost, H., Fnais, M., and Lelieveld, J.: Impact of mineral dust on cloud formation in a Saharan outflow region, Atmospheric Chemistry and Physics, 12, 11383-11393, 10.5194/acp-12-11383-2012, 2012.

Sokolik, I. N., Winker, D. M., Bergametti, G., Gillette, D. A., Carmichael, G., Kaufman, Y. J., Gomes, L., Schuetz, L., and Penner, J. E.: Introduction to special section: Outstanding problems in quantifying the radiative impacts of mineral dust, J. Geophys. Res.-Atmos., 106, 18015-18027, 10.1029/2000jd900498, 2001.

Solomos, S., Kushta, J., and Kallos, G.: Effects of Airborne Particles on Cloud Formation and Precipitation: A Modeling Study, in: Air Pollution Modeling and Its Application XXI, edited by: Steyn, D. G., and Castelli, S. T., NATO Science for Peace and Security Series C-Environmental Security, 571-578, 2012.

Streets, D. G., Bond, T. C., Carmichael, G. R., Fernandes, S. D., Fu, Q., He, D., Klimont, Z., Nelson, S. M., Tsai, N. Y., Wang, M. Q., Woo, J. H., and Yarber, K. F.: An inventory of gaseous and primary aerosol emissions in Asia in the year 2000, J. Geophys. Res.-Atmos., 108, 8809, 10.1029/2002jd003093, 2003.

Sun, H., Pan, Z., and Liu, X.: Numerical simulation of spatial-temporal distribution of dust aerosol and its direct radiative effects on East Asian climate, J. Geophys. Res.-Atmos., 117, D13206, 10.1029/2011jd017219, 2012.

Tong, D. Q., Bowker, G. E., He, S., Byun, D. W., Mathur, R., Gillette, D. A.: Development of a Windblown Dust Module within the Community Multi-scale Air Quality (CMAQ) Model: Description and Preliminary Applications in the Continental United States, the Journal of Geophysical Research, 2011 (submitted).

Wang, H., Zhang, X. Y., Gong, S. L., Chen, Y., Shi, G. Y., and Li, W.: Radiative feedback of dust aerosols on the East Asian dust storms, J. Geophys. Res.-Atmos., 115, D23214,10.1029/2009jd013430, 2010a.

Wang, K., Zhang, Y., Nenes, A., and Fountoukis, C.: Implementation of dust emission and chemistry into the Community Multiscale Air Quality modeling system and initial application to an Asian dust storm episode, Atmospheric Chemistry and Physics, 12, 10209-10237, 10.5194/acp-12-10209-2012, 2012a.

Wang, L. T., Jang, C., Zhang, Y., Wang, K., Zhang, Q., Streets, D., Fu, J., Lei, Y., Schreifels, J., He, K., Hao, J., Lam, Y.-F., Lin, J., Meskhidze, N., Voorhees, S., Evarts, D., and Phillips, S.: Assessment of air quality benefits from national air pollution control policies in China. Part I: Background, emission scenarios and evaluation of meteorological predictions, Atmospheric Environment, 44, 3442-3448, 10.1016/j.atmosenv.2010.05.051, 2010b.

Wang, L. T., Xu, J., Yang, J., Zhao, X., Wei, W., Cheng, D., Pan, X., and Su, J.: Understanding haze pollution over the southern Hebei area of China using the CMAQ model, Atmospheric Environment, 56, 69-79, 10.1016/j.atmosenv.2012.04.013, 2012b.

Wang, S. X., Zhao, M., Xing, J., Wu, Y., Zhou, Y., Lei, Y., He, K., Fu, L., and Hao, J.: Quantifying the Air Pollutants Emission Reduction during the 2008 Olympic Games in Beijing, Environmental Science & Technology, 44, 2490-2496, 10.1021/es9028167, 2010c.

Whitten, G. Z., Heo, G., Kimura, Y., McDonald-Buller, E., Allen, D. T., Carter, W. P. L., and Yarwood, G.: A new condensed toluene mechanism for Carbon Bond CB05-TU, Atmospheric Environment, 44, 5346-5355, 10.1016/j.atmosenv.2009.12.029, 2010.

Xiu, A. J., and Pleim, J. E.: Development of a land surface model. Part I: Application in a mesoscale meteorological model, Journal of Applied Meteorology, 40, 192-209, 10.1175/1520-0450(2001)040<0192:doalsm>2.0.co;2, 2001.

Yan, H., Gao, H., Yao, X., and Wang, Z.: Simulating dry deposition fluxes of PM10 and particulate inorganic nitrogen over the eastern China seas during a severe Asian dust event using WRF-Chem model, Journal of Ocean University of China, 11, 301-314, 10.1007/s11802-012-1857-2, 2012.

Ying, Z., Tie, X., Madronich, S., Li, G., and Massie, S.: Simulation of regional dust and its effect on photochemistry in the Mexico City area during MILAGRO experiment, Atmospheric Environment, 45, 2549-2558, 10.1016/j.atmosenv.2011.02.018, 2011.

Zender, C. S., Bian, H. S., and Newman, D.: Mineral Dust Entrainment and Deposition (DEAD) model: Description and 1990s dust climatology, J. Geophys. Res.-Atmos., 108, 4416, 10.1029/2002jd002775, 2003.

Zhang, X. Y., Gong, S. L., Zhao, T. L., Arimoto, R., Wang, Y. Q., and Zhou, Z. J.: Sources of Asian dust and role of climate change versus desertification in Asian dust emission, Geophysical Research Letters, 30, 2272, 10.1029/2003gl018206, 2003.

Zhang, Y., Liu, P., Pun, B., and Seigneur, C.: A comprehensive performance evaluation of MM5-CMAQ for the Summer 1999 Southern Oxidants Study episode - Part I: Evaluation protocols, databases, and meteorological predictions, Atmospheric Environment, 40, 4825-4838, 10.1016/j.atmosenv.2005.12.043, 2006.

Zhao, B., Wang, S. X., Wang, J. D., Fu, J., Liu, T. H., Xu, J. Y., Fu, X., Hao, J. M.: Impact of national NO_X and SO_2 emission control policies on particulate matter pollution in China, Atmospheric Environment, 77, 453-463, 2013.

Tables

Table 1. The emissions of major pollutants for each domain during 28 April to 6 May

	Unite	Domain1	Domain2	Domain3
PM_{10}	10^3t	543.6	329.7	28.5
$PM_{2.5}$	10^3t	399.2	230.9	15.3
SO_2	10^3t	706.6	501	36.5
NO_X	10^3t	571.5	395.7	56.4
NH_3	10^3t	432.7	276.1	30.1
VOC	10^9mol	55	25.1	4

Table 2. Scenario design for model simulations

Run Index	Model Configuration	Purpose
DUST_DEFAULT	The default parameters in the official version was used. (e.g. $u'_{*ti,j} \approx 0.7$ averagely and $PM_{2.5}/PM_{10}$=0.2)	Performance evaluation of the default dust model
DUST_REVISED	The threshold friction velocity for loose, fine-grained soil with low surface roughness and $PM_{2.5}/PM_{10}$ ratio are chosen based on Chinese data ($u'_{*ti,j} \approx 0.3$ and $PM_{2.5}/PM_{10}$=0.1)	Performance evaluation of the revised version
DUST_OFF	The dust model was turned off	Analysis of dust impacts

Table 3. Performance statistics of meteorological variables

			Domain 1	Domain 2	Domain3	Benchmark
Wind Speed (WS10)	Mean OBS	(m s^{-1})	3.53	3.26	3.50	
	Mean SIM	(m s^{-1})	3.48	3.23	3.29	
	Bias	(m s^{-1})	-0.05	-0.03	-0.21	≤±0.5
	GE	(m s^{-1})	1.35	1.21	0.99	≤2
	RMSE	(m s^{-1})	1.82	1.69	1.35	≤2
	IOA		0.82	0.80	0.83	≥0.6
Wind Direction (WD10)	Mean OBS	(deg)	231	195	129	
	Mean SIM	(deg)	220	200	128	
	Bias	(deg)	2.5	3.4	1	≤±10
	GE	(deg)	42	38	28	≤30
Temperature (T2)	Mean OBS	(K)	288.2	292.2	292.2	
	Mean SIM	(K)	286.3	291.4	290.8	
	Bias	(K)	-1.9	-0.8	-1.4	≤±0.5
	GE	(K)	2.9	2.0	2.3	≤2
	RMSE	(K)	5.8	3.1	2.8	
	IOA		0.88	0.95	0.87	≥0.8
Humidity (H2)	Mean OBS	(g kg^{-1})	6.88	10.13	9.63	
	Mean SIM	(g kg^{-1})	6.95	10.12	9.11	
	Bias	(g kg^{-1})	0.07	-0.01	-0.52	≤±1
	GE	(g kg^{-1})	1.42	1.76	1.41	≤2
	RMSE	(g kg^{-1})	13.93	11.69	1.95	
	IOA		0.31	0.63	0.66	≥0.6

Table 4. Model performance forhourlyPM_{10} concentrations

		Domain 1	Domain2	Domain3
	Number of stations	546	405	82
	Mean Obs.(μg/m^3)	119	127	176
DUST_OFF	Mean Sim.(μg/m^3)	63	79	49
	Bias(μg/m^3)	-56	-48	-127
	NMB(%)	-47.1	-37.8	-72.2
	R	0.05	0.04	0.05
DUST_DEFAULT	Mean Sim.(μg/m^3)	64	81	51
	Bias(μg/m^3)	-55	-46	-125
	NMB(%)	-46.2	-36.2	-71
	R	0.07	0.06	0.13
DUST_REVISED	Mean Sim.(μg/m^3)	106	136	152
	Bias(μg/m^3)	-13	9	-24
	NMB(%)	-10.9	7.1	-13.6
	R	0.42	0.46	0.63

Figure Caption

Fig.1.Modeling domains and location of the monitoring sites used for model evaluation.

Fig.2. Comparison of simulated PM_{10} concentration (a, c, e) and $PM_{2.5}$ concentration (b, d, f) with observations at three sites in the YRD

Fig.3 Comparison of simulated daily average AOD with observations at two AERONET sites, 28 April to 6 May

Fig.4. Distribution of daily mean dust PM_{10} emissions by DUST_REVISED model

Fig.5. The temporal variation of dust emissions

Fig.6.Surface and 500 hPa weather chart in China

Fig.7. Surface meteorological variables from May 1 to 6 in Shanghai monitoring site

Fig.8.The spatio-temporal variation of dust impacts on PM_{10} concentration ($\mu g/m^3$) in the surface layer during this dust event (DUST_REVISED minus DUST_OFF)

Fig.9. The PM_{10} deposition in the YRD region from 1 to 6 May

Fig.10. The average differences of the aerosol optical depth (AOD) at 550nm and downward irradiance simulated by DUST_REVISED and DUST_OFF, April 28 to May 6

Fig. 11 The average differences of the photolysis rates simulated by DUST_REVISED and DUST_OFF, April 28 to May 6

Fig.12 Diurnal cycle of the percentage change of the NO2 photolysis rate and the O3 photolysis rate at Shanghai, May 1 to May 3

Fig.13. The average differences between the simulations in the surface layer by DUST_REVISED and DUST_OFF, April 28 to May 6. (a)O3 concentrations;(b)OH concentrations

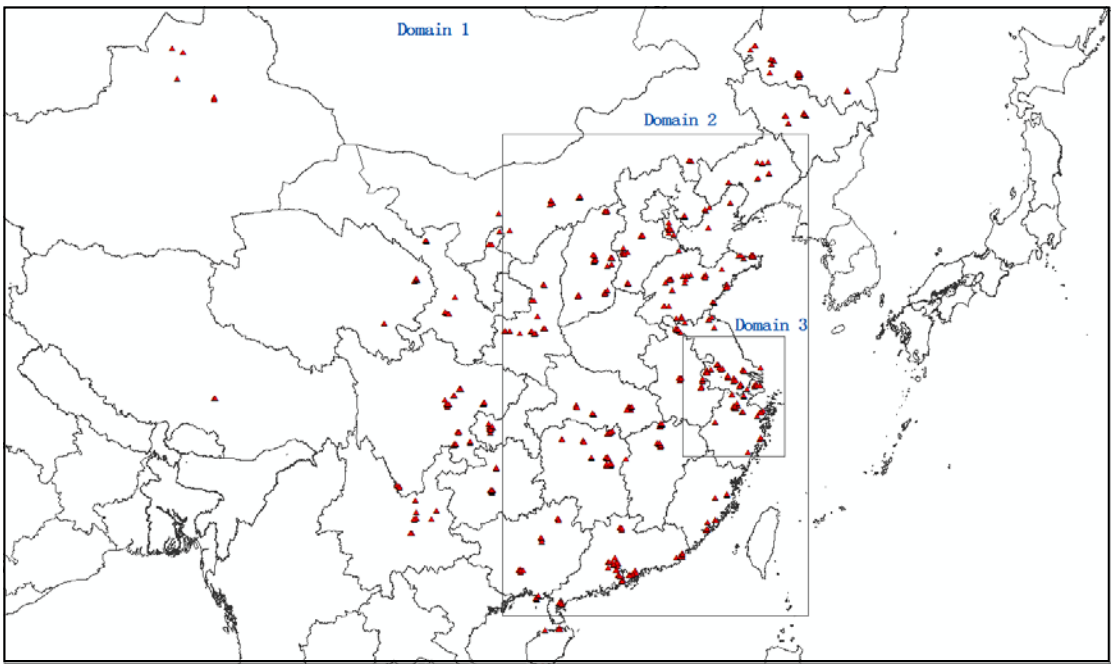

Fig.1. Modeling domains and location of the monitoring sites used for model evaluation. The red triangles indicate the 546 monitoring sites from the Ministry of Environmental Protection of China.

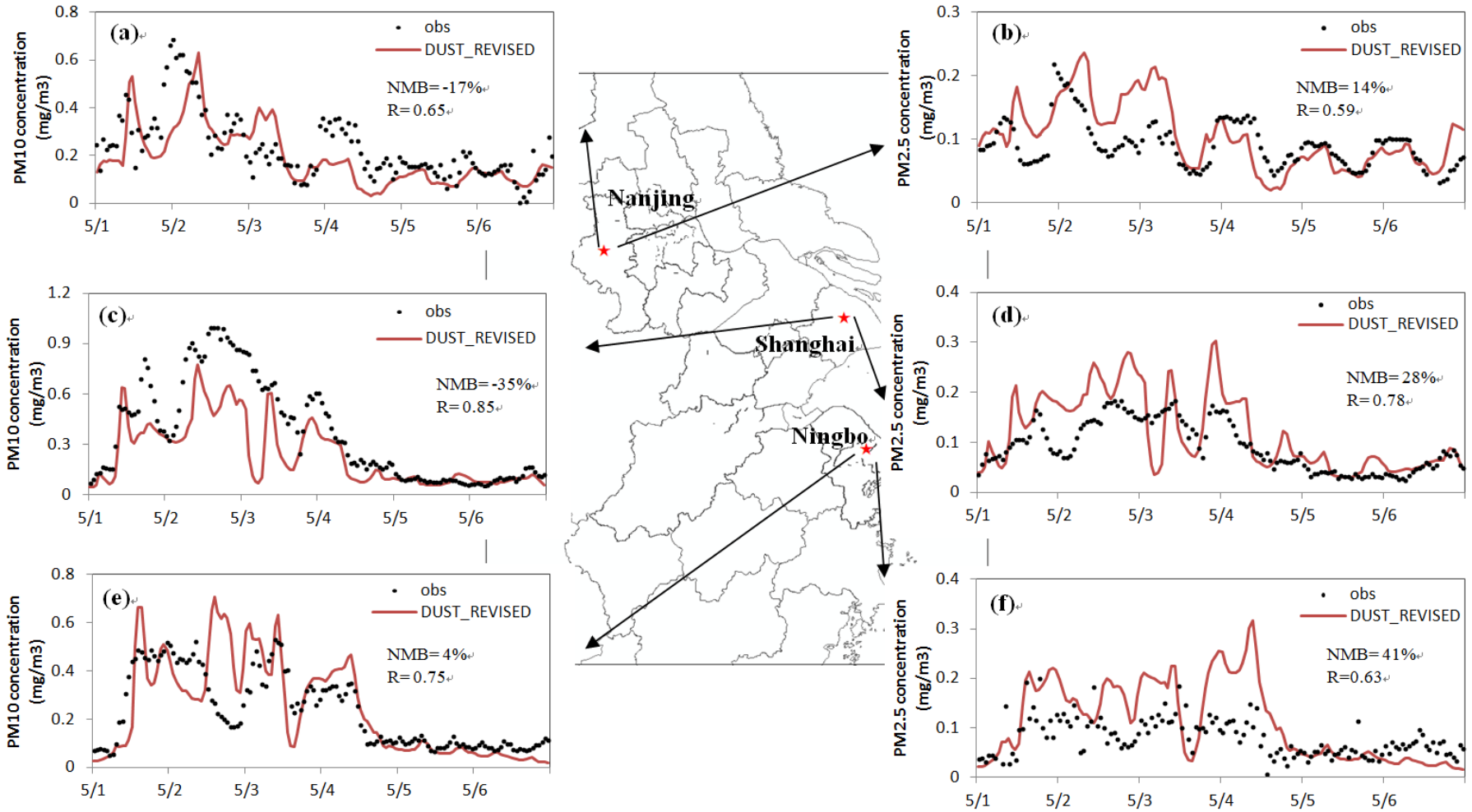

Fig.2. Comparison of simulated PM_{10} concentration (a, c, e) and $PM_{2.5}$ concentration (b, d, f) with observations at three sites in the YRD

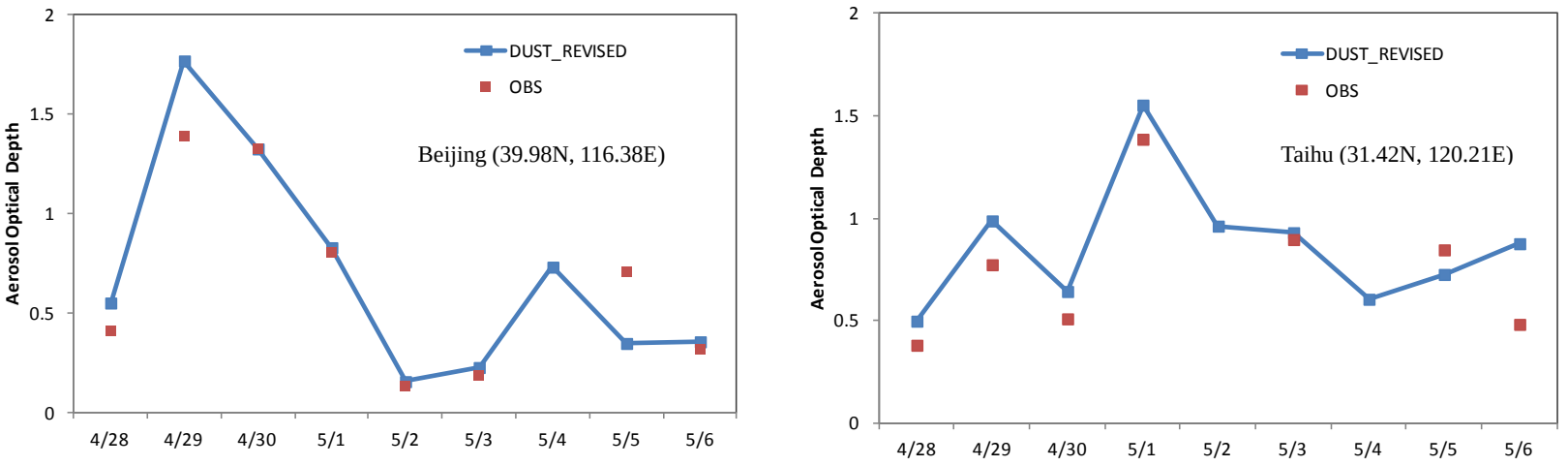

Fig.3 Comparison of simulated daily average AOD with observations at two AERONET sites, 28 April to 6 May

(a) April 28, 2011

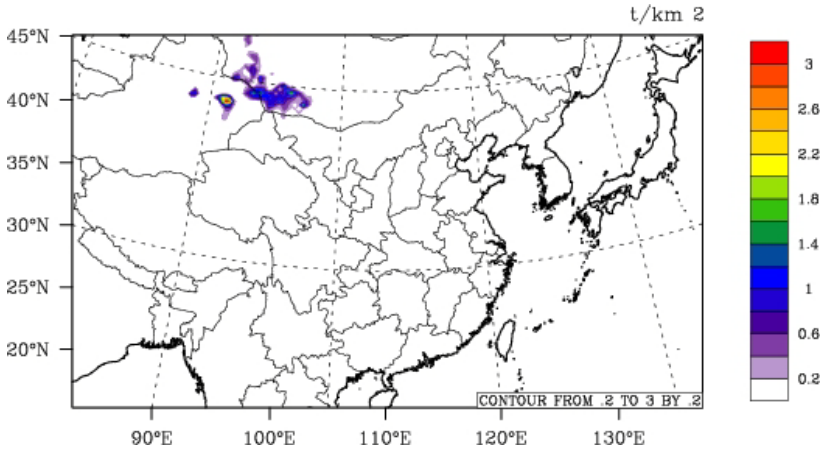

(b) April 29, 2011

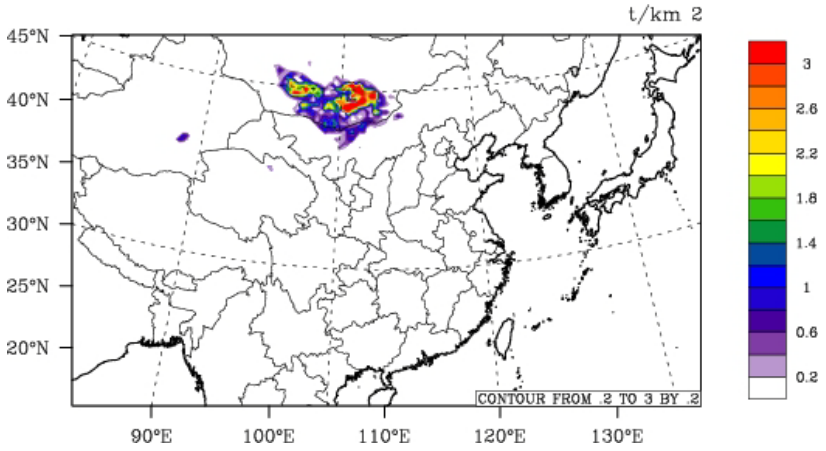

(c) April 30, 2011

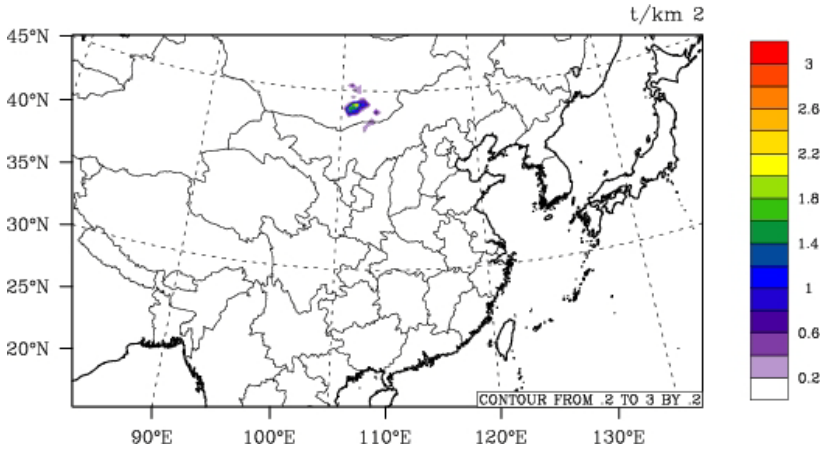

Fig.4. Distribution of daily mean dust PM_{10} emissions by DUST_REVISED model

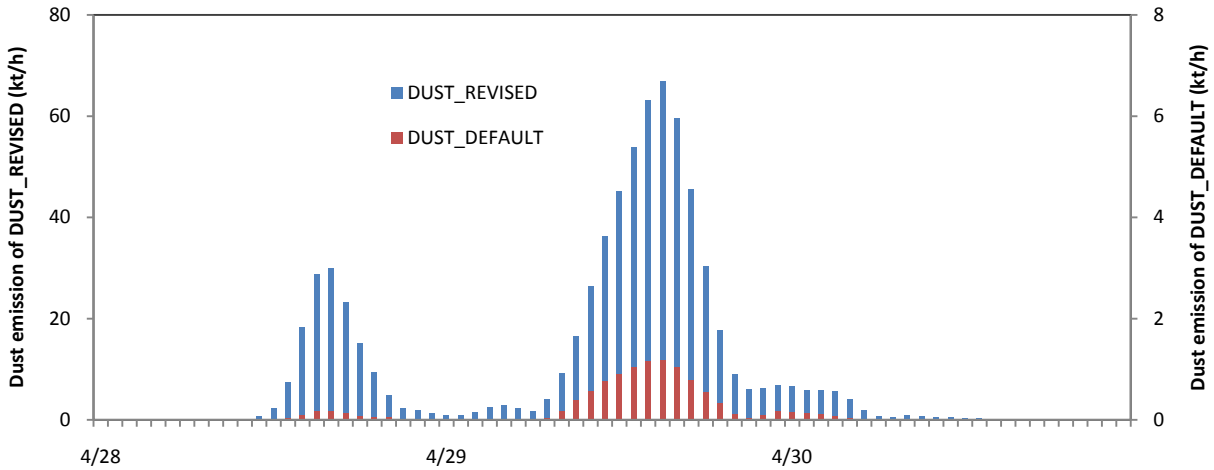

Fig.5. The temporal variation of dust emissions

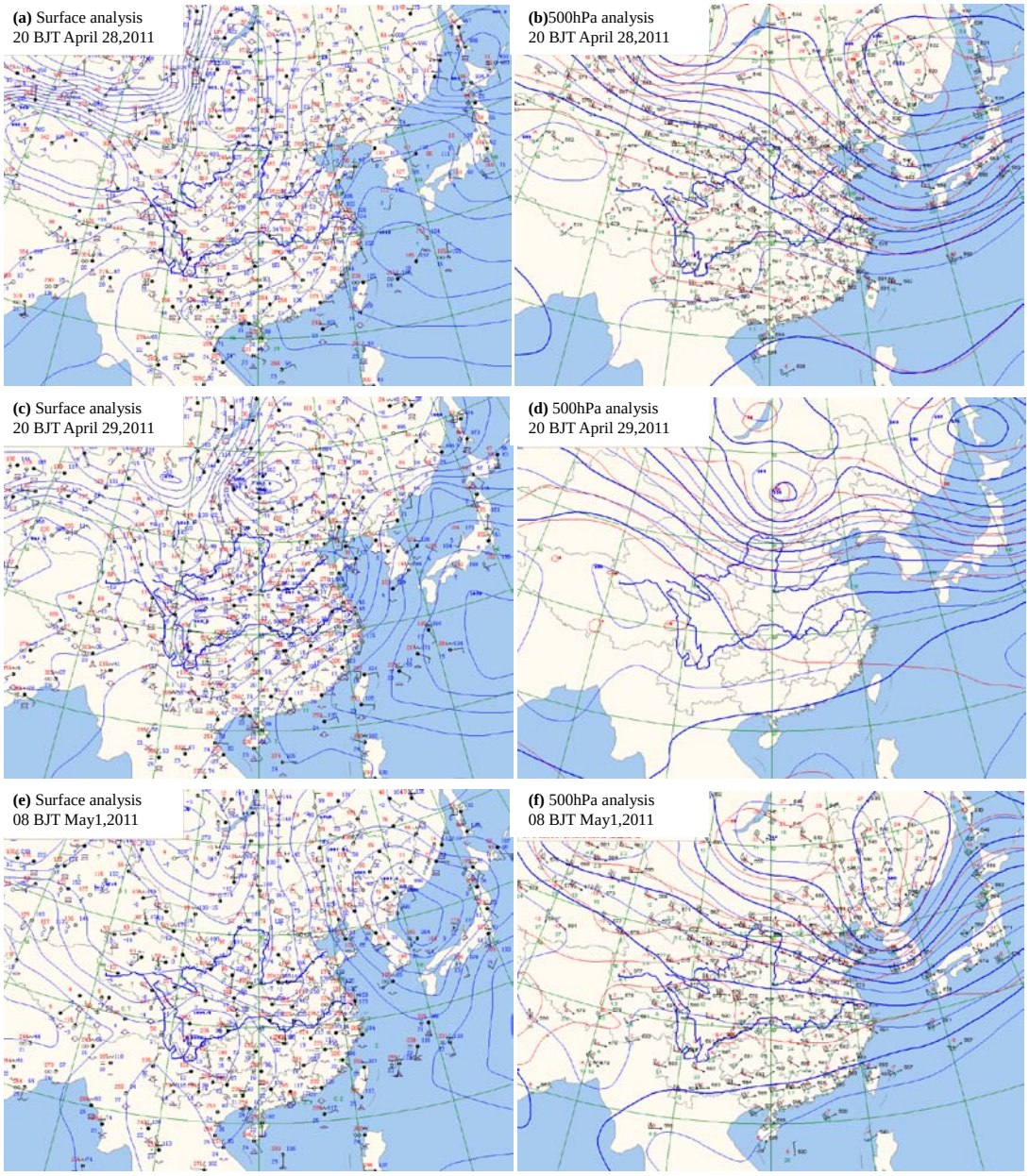

Fig.6. Surface and 500 hPa weather chart in China (http://218.94.36.199:5050/dmsg/map.htm)

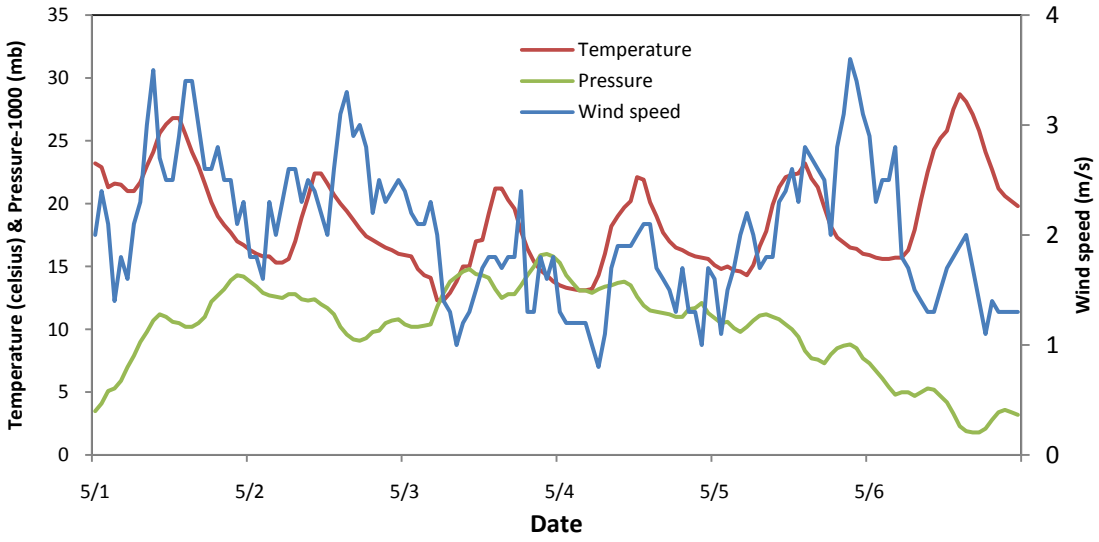

Fig.7. Surface meteorological variables from May 1 to 6 in Shanghai monitoring site

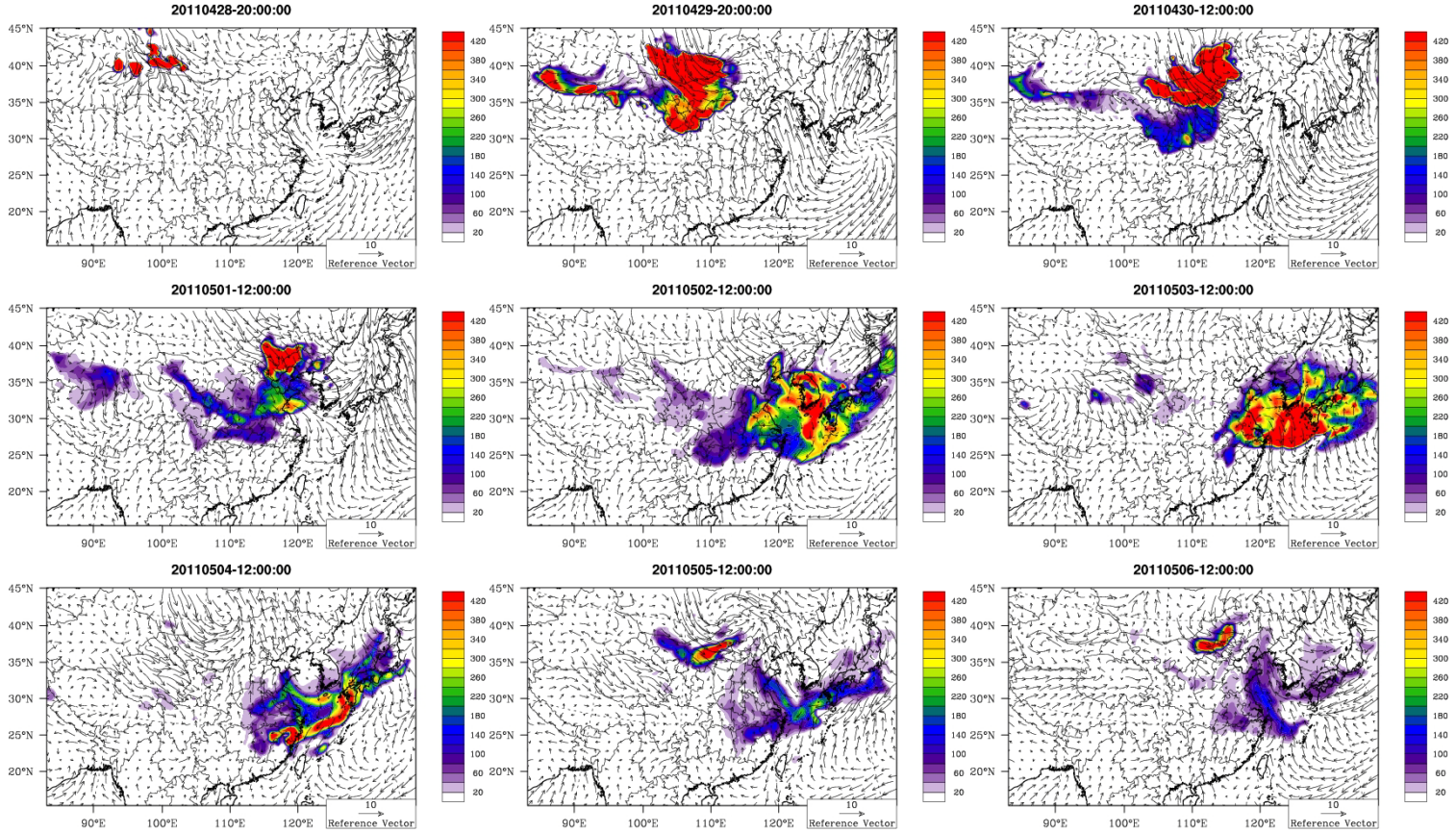

Fig.8. The spatio-temporal variation of dust impacts on PM_{10} concentration ($\mu g/m^3$) in the surface layer during this dust event (DUST_REVISED minus DUST_OFF)

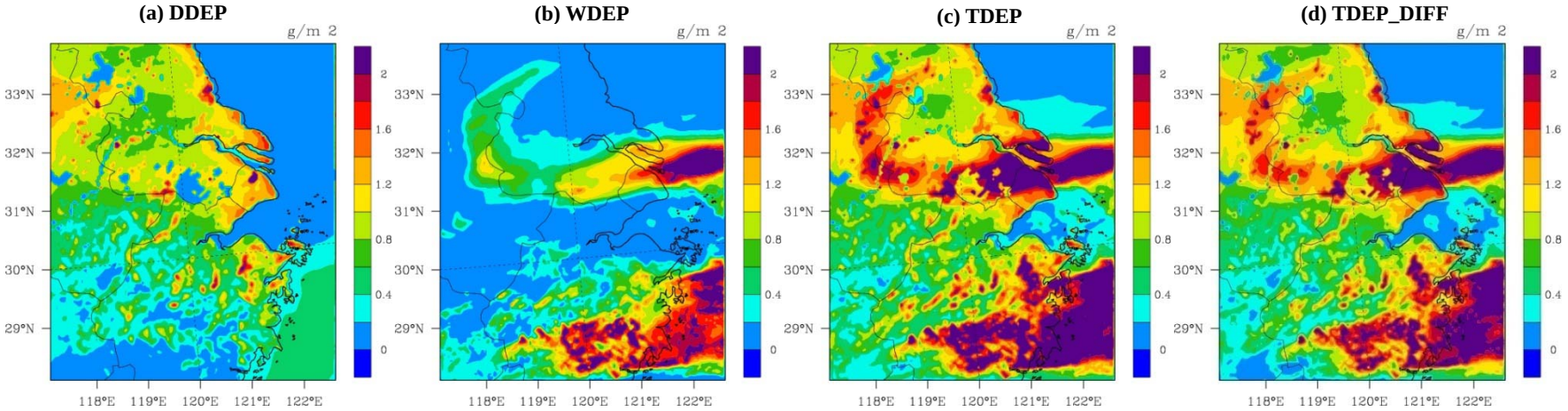

Fig.9. The PM_{10} deposition in the YRD region from 1 to 6 May

(a) Aerosol optical depth

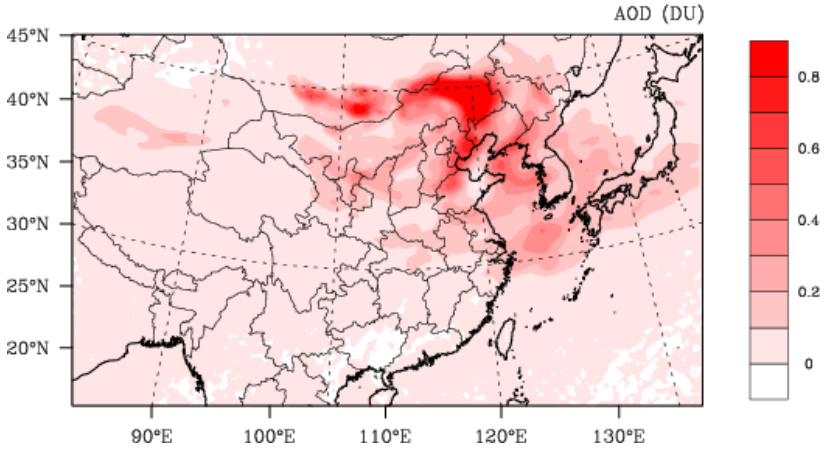

Fig.10. The average differences of the aerosol optical depth (AOD) at 550nm and downward irradiance simulated by DUST_REVISED and DUST_OFF, April 28 to May 6

(a) The NO_2 photolysis rate

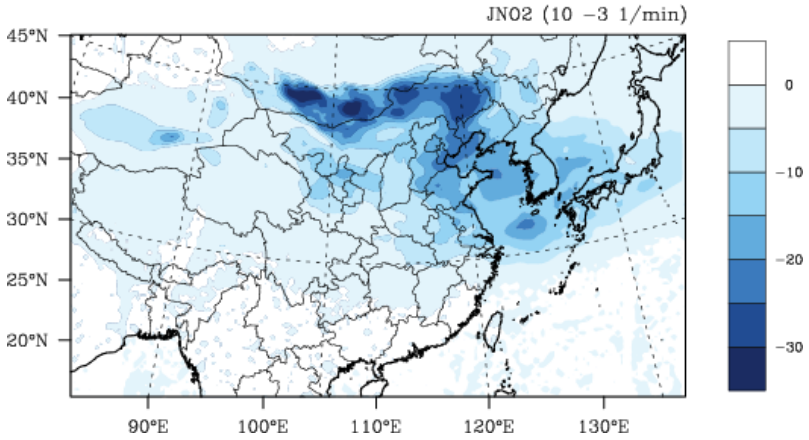

(b) The O_3 photolysis rate

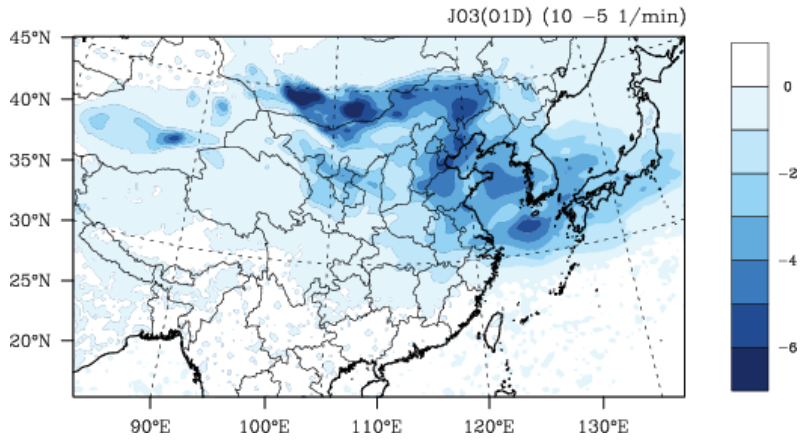

Fig. 11 The average differences of the photolysis rates simulated by DUST_REVISED and DUST_OFF, April 28 to May 6

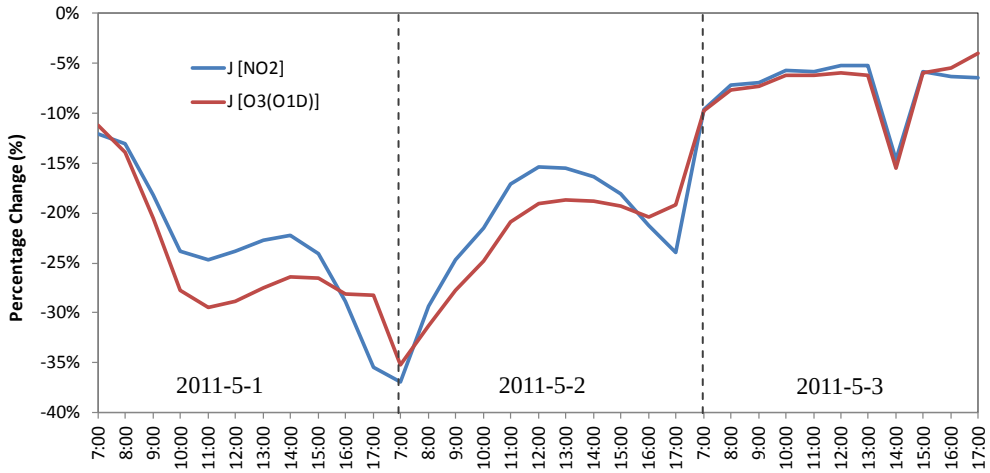

Fig.12 Diurnal cycle of the percentage change of the NO_2 photolysis rate and the O_3 photolysis rate at Shanghai, May 1 to May 3

(a) O_3 concentrations

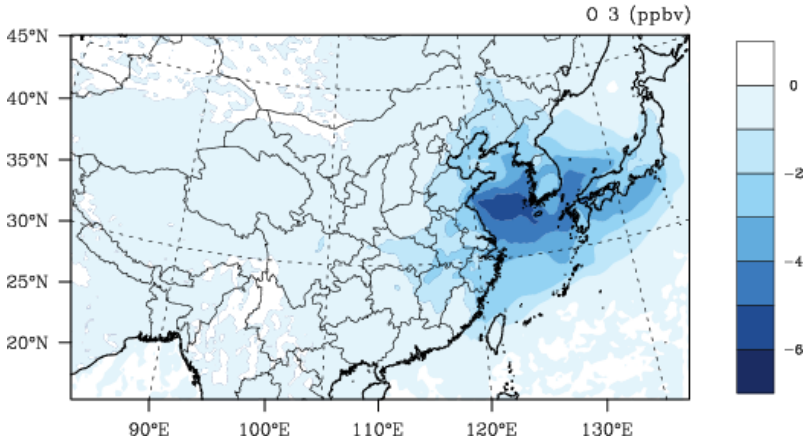

(b) OH concentrations

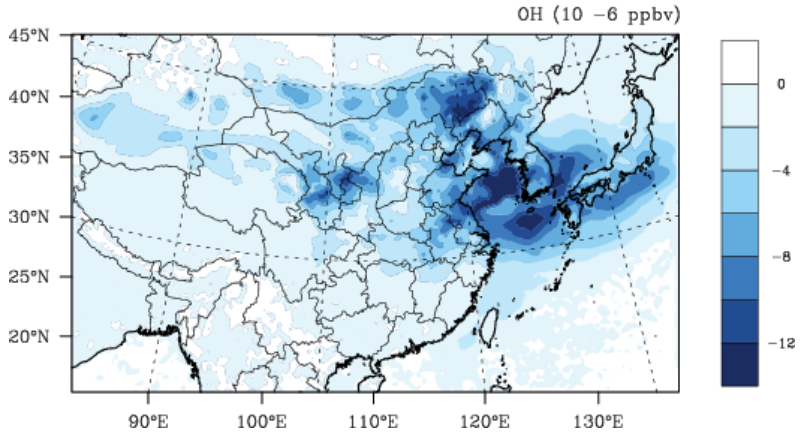

Fig.13. The average differences between the simulations in the surface layer by DUST_REVISED and DUST_OFF, April 28 to May 6. (a)O_3 concentrations;(b)OH concentrations